Published in final edited form as:
Top Magn Reson Imaging. 2008 February ; 19(1): 59–68. doi:10.1097/RMR.0b013e318176c57b.

Molecular Imaging in Cardiovascular Magnetic Resonance Imaging: *Current Perspective and Future Potential*

David E. Sosnovik, MD, FACC
From the Center for Molecular Imaging Research, and Department of Cardiology, Massachusetts General Hospital, Harvard Medical School, Boston MA

Abstract

The development of novel imaging agents and techniques is allowing some biological events to be imaged in vivo with magnetic resonance imaging (MRI) at the cellular and subcellular level. In this paper, the use of novel gadolinium chelates and superparamagnetic iron oxide nanoparticles for molecular MRI of the cardiovascular system is extensively reviewed. The physical properties of these imaging agents and the pulse sequences best suited to their visualization are extensively discussed. The application of molecular MRI in diseases of the vasculature and myocardium is then reviewed. The clinical experience to date, as well as the promise and potential impact of molecular MRI, is extensively discussed.

Keywords

magnetic resonance imaging; molecular imaging; cardiovascular; iron oxide; nanoparticles; myocardium; atherosclerosis

Molecular magnetic resonance imaging (MRI) refers to the noninvasive imaging of events at the cellular and subcellular level with MRI in vivo. Although the experience to date with nuclear-based molecular imaging techniques is greater, the advantages of an MRI-based approach to cardiovascular imaging include its high spatial resolution, excellent soft tissue contrast, and ability to simultaneously image cardiovascular anatomy, physiology, and molecular events.[1] Molecular MRI is already playing an important role in preclinical investigation and has the potential to play a major role in the clinical arena in the near future.[1] The present paper focuses on the role of MRI in cardiovascular molecular imaging, and the interested reader is referred to several broad reviews of the field for a more detailed discussion of other molecular imaging modalities as well.[1–3]

MOLECULAR MRI AGENTS

The principal challenge of molecular MRI, in comparison with other molecular imaging techniques such as single photon emission computed tomography/positron emission tomography (PET) and fluorescence, lies in its lower sensitivity. Conventional gadolinium chelates have a sensitivity in the micromolar range, which is significantly better than iodinated contrast agents (millimolar range) but significantly worse than radiotracer and fluorescence techniques (picomolar or better).[1,3,4] Two approaches have been developed to deal with this problem. The first involves the selection of highly expressed molecular targets, such as fibrin in thrombi or type 1 collagen in areas of fibrosis.[5,6] Because these targets are so abundant,

Reprints: David Sosnovik, MD, FACC, Center for Molecular Imaging Research, Massachusetts General Hospital, 149 13th St, Charlestown MA 02129 (e-mail: sosnovik@nmr.mgh.harvard.edu).

small gadolinium chelates with relatively low relaxivity values can be used for their detection. These agents are also similar in size to clinically approved gadolinium chelates, simplifying some aspects of their pharmacokinetic and toxicological evaluation. The principal disadvantage of this approach, however, lies in its low sensitivity per binding event (low level of signal generated for each unit ligand that binds to the target). This limits the applicability of this approach to highly expressed targets and also requires a large amount of the targeting ligand to be synthesized.

The second approach involves the synthesis of novel MRI agents that have significantly higher relaxivities than conventional gadolinium chelates.[1] These agents include gadolinium-containing liposomes, lipoproteins and micelles,[7–10] and superparamagnetic iron oxide magnetic nanoparticles (MNPs).[11,12] These agents contain thousands of gadolinium or iron atoms for each targeting ligand attached to their surface, producing a high level of detection efficiency for each binding event. The high relaxivities of these agents, particularly superparamagnetic iron oxide MNPs, also play a vital role in allowing them to detect sparsely expressed targets in the low nanomolar range.[13–15] The cost of this greater detection sensitivity, however, lies in the larger size and more complex pharmacokinetics of these agents, particularly the gadolinium-containing liposomes and micelles.

Liposomes and micelles that are heavily loaded with paramagnetic gadolinium chelates have longitudinal relaxivity (R1) values[9,13] ranging from 10 to 20 s^{-1}·mmol/L^{-1}. The relaxivity of a magnetic resonance (MR) contrast agent reflects its ability to interact with adjacent protons and strongly influences its detectability. The higher the longitudinal relaxivity (R1) of an agent, the brighter the tissue in its vicinity becomes on a T1-weighted image, whereas the higher the transverse relaxivity (R2), the darker the tissue becomes on a T2-weighted image. Gadolinium-based probes are generally imaged with T1-weighted sequences at standard clinical field strengths, producing positive contrast.

Initial studies with a novel molecular imaging agent are frequently done in mice because of the relatively low amount of the experimental agent that needs to be synthesized for each animal. An equal amount of the contrast agent and targeting ligand, for instance, needs to be synthesized to image 1 rabbit and 100 mice. Cardiovascular MRI studies in mice, however, are best performed at high field strengths (7 T and higher) to allow the small cardiovascular structures to be imaged with adequate spatial resolution and signal to noise.[16] However, the R1 of gadolinium-containing paramagnetic agents can decrease with increasing field strength, reducing the sensitivity of these probes at high field.[13] Higher doses of a gadolinium-containing imaging agent may thus be needed to image a given target in mice at 7 T than in humans at 1.5 to 3 T.[13]

Iron oxide MNPs are typically superparamagnetic and can be imaged with T1, T2, T2*, off resonance, and steady-state free precession (SSFP) techniques.[14,17–20] Magnetic nanoparticle agents have a central core of iron oxide, 3 to 5 nm in diameter, surrounded by a carbohydrate or polymer coat.[11,12] Selected MNP have been used extensively in the clinical arena to image the liver and lymphatic system,[21] and their established safety record thus makes them a highly appealing platform for molecular MRI. The R2 values[12,22] of these agents range from 50 to greater than 600 s^{-1}·mmol/L^{-1} and remain constant over all field strengths greater than 0.5 T.[19] However, the R1 values and, in particular, the R1/R2 values of these agents decrease with increasing field strength.[19] T1 contrast can thus be achieved with MNPs at conventional clinical field strengths (1.5–3 T)[17]; however, at higher strengths, the R2 effects of the probe dominate its R1 effects even at fairly short echo times (TEs). Imaging of MNPs in mice tends to be done at high field strengths, for the reasons alluded to above, and it is thus usually performed with a T2 or T2* approach. The sensitivity of a T2- or T2*-based approach for the detection of MNP at 1.5 to 3 T, however, is equal to that achieved for the detection of

MNP in mice at 7 to 15 T because the R2 and R2* values of these super-paramagnetic agents saturate and stay constant above 0.5 T. A shorter TE, however, is required for a given degree of T2/T2* weighting at higher field strengths, which can be helpful when dealing with rapid heart rates and, hence, rapidly moving structures.

First-generation MNPs, such as Feridex (Advanced Magnetics, Cambridge, Mass), contain relatively thin dextran coats and tend to form polycrystalline clusters, which are rapidly cleared from the bloodstream by the reticuloendothelial system. Feridex has thus been Food and Drug Administration–approved for the detection of liver masses after intravenous injection since 1993. The metabolism, pharmacokinetics, and toxicity of MNPs taken up by cells in the reticuloendothelial system have been well studied,[23] and no toxic effects related to MNP administration have been found. Iron radiotracer (59Fe) and MR relaxivity studies have also shown that the iron oxide core of the MNP is broken down into other forms of iron and then incorporated normally into hemoglobin in newly forming erythrocytes.[23] The pharmacokinetics, metabolism, and safety profile of Feridex when used to load stem cells for MR-based tracking, however, requires a full safety evaluation in each case.

Second- and third-generation MNP have been synthesized with more extensive polymer coatings and remain monodisperse in solution.[11] These agents have a much longer blood half-life (24 hours in humans, 11 hours in mice) and typically have a homogenous size distribution in the 30- to 50-nm range.[11,12,24] The small size, long blood half-life, and high relaxivities of these MNP constitute a powerful combination that allows them to penetrate deep tissue spaces, such as the interior of atherosclerotic plaque and the myocardium,[25,26] and detect sparsely expressed targets in the low nanomolar range. A highly stabilized and cross-linked derivative of monocrystalline iron oxide (MION), known as cross-linked iron oxide (CLIO), has also recently been developed for targeted molecular imaging applications.[12,24] Cross-linked iron oxide contains aminated cross-linked dextran chains, allowing a large variety of ligands to be conjugated to the nanoparticle with a high degree of stability and relative ease. Near-infrared fluorochromes, for instance, can be attached to the amine groups on the probe to form a dual modality magnetofluorescent nanoparticle.[27,28] In addition, several copies of the targeting ligand can subsequently be attached to the CLIO-fluorochrome conjugate to form a multivalent (>1 targeting ligand) magnetofluorescent nanoparticle.

Molecular MR agents can be targeted through the attachment to their surface of an affinity ligand (antibody, fragments, proteins, peptides, and aptamers) directed against a known target on the cell surface, such as the $\alpha_v\beta_3$ integrin,[29,30] phosphatidylserine,[28,31] or vascular cell adhesion molecule (VCAM)-1.[15,32] Alternatively, the surface of the MNP can be modified with small molecules to modulate its uptake.[33,34] Although these small chemical moieties are several orders of magnitude smaller than the MNP, they strongly influence the binding and in vivo kinetics of the probe through mechanisms such as surface charge. Surface-modified MNPs that are highly specific for either resting or activated macrophages have, for instance, been identified in a high-throughput chemical screen.[33] Magnetic nanoparticle may thus be targeted not only to cell type but also to cell state. Coating an MNP with the small chemical succinimidyl iodoacetate can dramatically reduce its uptake by both resting and activated macrophages.[33] This suggests that the uptake of MNPs such as MION and CLIO by macrophages is more complex than initially thought and not simply an automatic consequence of a macrophage encountering a synthetic nanoparticle.[33]

The size and physical characteristics of molecular MR contrast agents significantly influence their pharmacokinetics. Large liposomes are limited to the intravascular space, whereas smaller liposomes may be able to access the interstitial space. Gadolinium constructs with hydrophobic groups, such as gadofluorine, may show preferential accumulation in areas of atherosclerotic plaque.[35] This agent, however, can also bind nonspecifically to structures in the interstitial

space and become trapped in the extracellular matrix.[36] The blood half-life of a gadolinium-containing micelle or liposome may thus be relatively short, but its tissue elimination half-life may be significantly longer. The implications of this will need to be carefully studied, given the recent experience with inadequate gadolinium elimination in nephrogenic systemic fibrosis.

Magnetic nanoparticles do not react with elements of the interstitial space but can be taken up by monocytes infiltrating injured tissue.[25,26] This can be advantageous and be used to image inflammation but can also limit the specificity of targeted imaging with MNPs in tissues that have become highly infiltrated by macrophages. In tissues without a significant macrophage infiltrate, ligand-mediated binding of an MNP to either the cell surface or an appropriate receptor often results in their internalization into the cell.[32,37] Once within the cell, the MNPs become trapped and compartmentalized within lysosomes producing strong biological amplification of the signal.[37] This amplification is due to an increase in R2 when a given concentration of MNP becomes compartmentalized or aggregated rather than remaining disperse in solution[38] and forms the basis of the magnetic relaxation switches developed for in vitro bioassays.[39] Although some limitation on the frequency of MNP administration will be needed to avoid iron overload, it is likely that the lysosomes of cells that internalize MNPs will be able to break them down and release the iron into the general body pool for either excretion in the bile or synthesis of new hemoglobin.[23]

IMAGING TECHNIQUES

The ability of molecular MR contrast agents with high relaxivities to detect sparsely expressed targets has been well documented with a variety of techniques.[13–15] Gadolinium-based probes are usually imaged with T1-weighted sequences, whereas T2*-weighted and SSFP sequences have proven most sensitive for the detection of MNP.[14,15,18] When the diffusion of water is completely unrestricted, the sensitivity of T2-weighted imaging for MNP approaches that of T2*-weighted imaging. Diffusion in the vessel wall or myocardium, however, is usually significantly restricted, and a T2*-weighted approach is thus more sensitive. Steady-state free precession imaging has been used in a clinical system fitted with high-performing animal gradients and was able to image single cells loaded with MNP in the brain.[40] It is unlikely, however, that this degree of sensitivity will be reached in the thorax where motion and B0 inhomogeneity are both significantly more profound.

Steady-state free precession imaging forms the backbone of most cardiac MRI studies and produces significantly better image quality than gradient echo techniques. Tissue contrast in SSFP, however, is a combination of T2 and T1 effects and is highly nonlinear, being heavily influenced by, among other factors, the echo spacing in the sequence. When the resonance offset angle of the steady-state magnetization approaches ±180 degrees, an abrupt and dramatic local loss of signal occurs. This phenomenon can be exploited to detect MNP but may also produce off-resonance artifacts in areas with no iron oxide, particularly at higher fields. The ability of SSFP sequences, including those with inversion or T2-preparation prepulses, to accurately and linearly quantify the accumulation of molecular imaging agents has not yet been conclusively shown. At the present time, therefore, T1- and T2*-weighted gradient echo or spin echo sequences should be considered the methods of choice for the detection of molecular MRI agents in the cardiovascular system.

T2, T2*, and SSFP sequences produce negative contrast or relative signal hypointensity near the MNP. Concerns have been raised, however, that this negative contrast can be nonspecific and difficult to discern from other causes of signal hypointensity such as calcification, susceptibility artifacts, and flow-related signal loss or air (Table 1). The linearity of T2*-based contrast has also been questioned, particularly in the area of stem cell imaging where the cells are often heavily loaded with large amounts of MNP. Off-resonance techniques that generate

positive contrast near the MNP have thus recently been developed in the hope of addressing some of these concerns.[19,20,41,42]

Positive contrast techniques include those that selectively excite off-resonance spins,[41] exploit saturation transfer from the off-resonance to the on-resonance proton pool, and modulate the slice rephasing gradient to fully rephase only those spins that experience additional rephasing from the dipole field generated by the MNP[42] and sequences that suppress on-resonance protons with either inversion recovery or chemical saturation techniques.[19,20] The sensitivity of these positive contrast sequences for MNP is generally less than T2* imaging but may approach low-nanomolar sensitivity when performed at low field, under optimal conditions and with parameters producing reduced specificity.[19,20,42] However, off-resonance techniques are inherently unsuited to imaging at higher field strengths because the on-resonance water linewidth broadens, producing a decrease in the spectral separation between the on- and off-resonance spins.[19] Another challenge with these techniques, and at high field in particular, seems to be the nonlinear response in signal intensity to MNP concentration.[19] As the MNP content in a voxel increases, the percentage of spins shifted off resonance increases, but the T2 of these shifted spins also becomes extremely short, counteracting the positive contrast.[19] The linearity of the positive contrast techniques particularly at high field strengths can thus become unpredictable, especially if the TE is not kept extremely short.

The average resonance shift induced at an air interface was recently shown to be approximately 300 Hz at 4.7 T, which corresponds to an off-resonance shift obtained with 150 μg Fe/mL of MNP.[19] The imaging of MNP with positive contrast techniques in regions of the body with complex air interfaces is thus complicated by this nonspecific shift, particularly at high field strengths where the shift is larger. Positive contrast techniques are thus likely to work best when high local concentrations of MNP are imaged at 1.5 to 3 T.[20,42,43] At these field strengths, the on-resonance linewidth is narrowest, and the nonspecific off-resonance shifts are lowest. Although positive contrast off-resonance techniques represent a useful adjunct to T1, T2, T2*, and SSFP imaging of MNP, a thorough knowledge of how to use them optimally and interpret the artifacts associated with their use is needed.

Molecular MRI in areas of the cardiovascular system with a low level of susceptibility artifacts can be robustly performed with conventional (negative contrast) T2*-weighted imaging. Such areas include most of the myocardium (septum and anterior and lateral walls) and the aortic root. Confirmation that the signal hypointensity is due to MNP accumulation can be obtained with T1-weighted and off-resonance imaging, if needed, particularly at standard clinical field strengths (Table 1). The inferior wall of the myocardium and much of the thoracic aorta, however, are prone to large susceptibility artifacts at their air interfaces. Magnetic nanoparticle in these areas may be better imaged with a T2-weighted approach and, at 1.5 to 3 T, by T1-weighted imaging too. Off-resonance techniques may be useful in these areas at lower fields, but caution must be exercised to ensure that the positive contrast is not due to susceptibility shifts arising at the air-tissue interface.[19]

T1-weighted images to detect gadolinium-based probes also need to be interpreted in the context of several potential artifacts (Table 2). Fat has a high R1 value and seems bright on T1-weighted sequences. Incomplete suppression of perivascular or epicardial fat, for instance, can mimic uptake of a gadolinium-based probe in the vessel wall or subepicardium. Slow flow within the vessel lumen or ventricle can result in incomplete suppression of the blood signal and, thus, also mimic uptake of the probe within the endothelium or subendocardium. At higher fields, B1 inhomogeneity can produce significant variations in signal intensity because of inconsistent flip angles.[44] B1 shimming, which requires multiple transmission coils and channels, may be required to address this if T1-weighted sequences are to be used optimally in humans and large animals at field strengths greater than 3 T.[44]

One of the traditional limitations of molecular imaging by MRI has been its ability to provide only a single composite readout of the proton signal and, thus, image only a single biological process at a given time. Both gadolinium and iron oxide MNPs have T1 and T2 effects. However, for a given field strength, if 2 distinct TEs can be found at which the R1 effects of gadolinium strongly outweigh its R2 effects, although the R1 and R2 effects of MNP are balanced, and the R2 effects of MNP strongly outweigh the R2 effects of gadolinium, then the signal due to the gadolinium-based probe and the MNP can potentially be approximately distinguished from each other. Given the imperfections and approximations needed for this approach, several strategies are currently being developed to image 2 distinct MR signals with greater precision. One such approach involves the combined use of proton and fluorine MRI.[45] The Larmor frequencies of protons and fluorine are close to each other, and no background fluorine signal is present in the body. However, even when fairly concentrated in labeled cells, the magnitude of the fluorine signal is significantly lower than that produced by equivalent proton-based probes,[46] limiting the sensitivity of fluorine MRI. An alternative approach to multispectral MRI is to exploit the magnetization transfer between 2 pools of protons with an offset in their Larmor frequencies, a concept that forms the basis of chemical exchange saturation transfer (CEST), paramagnetic CEST, and liposome-based CEST techniques.[47,48] These techniques, like fluorine MRI, are still at an investigational stage and may also lack sensitivity for sparsely expressed targets. However, the use of the CEST-based techniques and fluorine MRI could prove to be highly valuable, particularly at higher field strengths where their sensitivity is significantly increased.

APPLICATIONS: VASCULAR IMAGING

Molecular MRI can be used to detect several important components of atherosclerotic plaque including adhesion molecules, plaque hemorrhage, and plaque macrophage content.[1,2] Gadofluorine is a novel fluorinated chelate of gadolinium that is more lipophilic and has a longer circulation half-life than conventional chelates. In a rabbit model of atherosclerosis, gadofluorine accumulated preferentially in areas of atherosclerotic plaque (Fig. 1).[35,49] Recombinant high-density lipoprotein (HDL)–like nanoparticles containing gadolinium have also been shown to accumulate in atherosclerotic plaques (Fig. 1).[9] Furthermore, the rate of uptake of these HDL-like nanoparticles into plaques in apoE$^{-/-}$ mice correlated with the lipid and macrophage content of the plaque. Plaques with a high macrophage density tended to take up the probe quicker than those with a low macrophage content.[9]

Plaque macrophage imaging with MNP has been performed in humans, large animal models, and apoE$^{-/-}$ mice.[25,50–52] However, use of the magnetofluorescent nanoparticle CLIO-Cy5.5 in cholesterol-fed apoE$^{-/-}$ mice showed that, although most CLIO-Cy5.5 was taken up by plaque macrophages, activated smooth muscle and endothelial cells also ingested the probe but to a lesser extent.[25] A good correlation between in vivo visualization of MNP and the histological presence of macrophages has also consistently been found in large animal models and in humans.[50–52] More recently, a gadolinium-containing micelle decorated with an antibody targeted to the macrophage scavenger receptor has been used to image macrophages in atherosclerotic plaques in apoE$^{-/-}$ mice (Fig. 1).[10] A strong correlation between plaque macrophage content and MR contrast enhancement was seen.

Adhesion molecules are expressed on the endothelium early in the atherosclerotic process. The presence of angiogenesis in the adventitia has also been implicated in the pathophysiology of plaque inflammation and rupture. A gadolinium-containing liposome targeted to the $\alpha_v\beta_3$ integrin has been used to image the local increase in angiogenesis in a rabbit model of atherosclerosis.[8] The feasibility of a “theranostic” approach that combined targeted diagnostic imaging with the delivery of a therapeutic agent was demonstrated by incorporating the antiangiogenic agent fumagillin into the liposome.[8] Decreased uptake of the probe was seen

after a second injection of the agent 2 weeks later, indicating a reduction in plaque angiogenesis (Fig. 1).[8]

Several generations of MRI agents targeted to the VCAM-1 receptor have been developed, using the magneto-fluorescent nanoparticle CLIO-Cy5.5 as a platform. In the most recent generation of these probes, a phage-derived linear peptide was used to synthesize a probe with superior target affinity.[15] Using this probe, VCAM-1 expression could be successfully imaged with MRI in the aortic roots of live apoE$^{-/-}$ mice (Fig. 2).[15] In addition, the effect of statin treatment on VCAM-1 expression was imaged in vivo by demonstrating decreased accumulation of the VCAM-targeted agent in the aortic roots of statin-treated mice (Fig. 2). This VCAM-1–sensing iron oxide probe thus detected a sparsely expressed target and also demonstrated adequate dynamic range to detect a treatment effect.[15]

Molecular MRI of intraplaque hemorrhage can be imaged in several ways. An off-resonance technique has been used to detect endogenous ferritin in atherosclerotic plaques complicated by hemorrhage.[53] Agents directed against fibrin have also been used to image plaque rupture and thrombosis.[5,54] One such agent consists of a 6–amino acid peptide conjugated to a small gadolinium chelate.[5] This agent has been used to successfully image fibrin associated with experimental thrombosis in animals[5] (Fig. 1) and, more recently, to image thrombosis in several clinical patients as well.[55]

Molecular MRI of atherosclerotic plaque has the potential to complement and enhance the ability of conventional MRI techniques to characterize plaque. The imaging agents and techniques previously discussed have the potential to facilitate the early detection of atherosclerotic disease and the detection of those plaques prone to rupture and complication. The potential of combining a diagnostic and therapeutic agent in a single targeted nanoparticle is also highly appealing and feasible.[8] Although not yet optimal, MRI of the coronary arteries is steadily improving and will likely be able to robustly support molecular MRI of major portions of the coronary circulation in the near future.

APPLICATIONS: MYOCARDIUM

Targeted imaging with MNP-based probes in the myocardium currently needs to be performed during either acute (first 24 hours) or chronic (>2 weeks) phase of injury when the myocardium is not heavily infiltrated with macrophages. Cardiomyocyte apoptosis, for instance, has been imaged in vivo by MRI in a mouse model of acute reperfusion injury.[14] No significant changes were seen in myocardial signal intensity when the mice were injected with an unlabeled control probe. However, as shown in Figure 3, injection of an identical dose (2 mg Fe/kg) of the annexin-labeled probe (AnxCLIO-Cy5.5) produced significant negative contrast enhancement in the injured myocardium (Fig. 3).[14] T2* maps of the hypokinetic regions of the myocardium also showed significant differences in those mice given the active versus unlabeled probe (Fig. 3). The in vivo MRI results were further confirmed by fluorescence reflectance imaging of the near-infrared fluorochrome (Cy5.5) on the probe ex vivo.[14] Annexin-labeled liposomes have recently been used to detect apoptosis in an isolated rat heart after ischemia-reperfusion.[56] The small size of the liposome allowed it to penetrate into the interstitial space of the myocardium, but further experience will be needed with this construct to determine its efficacy in vivo. Cardiomyocyte necrosis has been imaged by MRI in the rat heart ex vivo with an antimyosin antibody conjugated to MION.[57] The use of this probe in conjunction with apoptosis-detecting probes could thus provide powerful insights into the pathogenesis of cell death during acute myocardial injury, transplant rejection, and myocarditis.

The properties of MNP make them ideal agents with which to image myocardial macrophage infiltration in healing infarcts, transplant rejection, and myocarditis.[26,58,59] In a recent study, mice were injected intravenously with 3 to 20 mg Fe/kg of the MNP, CLIO-Cy5.5, 48 hours

after the infarct and then imaged with conventional T2*-weighted MRI a further 48 hours later. Negative contrast, consistent with the uptake of the probe by infiltrating macrophages, was seen in the infarcted anterolateral myocardium of all mice and at all doses (Fig. 4).[26] The Food and Drug Administration–approved dose for intravenous injections of clinically used MNPs is 3 mg Fe/kg, and the ability of this experimental MNP, as well as AnxCLIO-Cy5.5, to be detected at a dose of 3 mg Fe/kg or less is thus highly encouraging. Contrast-to-noise was measured in the mice between the septum and the anterolateral wall and displayed a strong and linear relationship with the dose of MNP injected (Fig. 4).[26] An off-resonance sequence has also been used to image macrophage accumulation in this model (Fig. 4) but displayed lower sensitivity than the conventional T2*-based approach.[19]

The detection of inflammation in the myocardium can also be performed by imaging a myeloperoxidase-activated gadolinium chelate.[60] Myeloperoxidase is released by macrophages and causes the serotonin-gadolinium chelate to become activated, form dimers and oligomers, and thus increase its R1 value significantly.[60] The use of this probe has the potential to allow oxidative stress in the myocardium to be imaged in healing infarcts, myocarditis, and transplant rejection. Once the inflammatory phase myocardial injury has resolved, however, a significant amount of fibrosis often develops in the myocardium over time. A small gadolinium chelate labeled with a peptide specific to type 1 collagen has recently been shown to detect myocardial fibrosis in mice with chronic myocardial infarcts (Fig. 5).[6] Sustained enhancement in the infarct zone was seen when the chelate was labeled with the collagen-binding peptide but not when it was labeled with the isomer of the peptide (Fig. 5).[6] Initial studies suggest that this construct may be more sensitive for the detection of myocardial fibrosis than currently used gadolinium chelates, but this will require further study.[6]

Stem cell therapy to attenuate myocardial injury and regenerate injured myocardium is being intensively studied. Magnetic nanoparticle (principally Feridex) and, more recently, fluorine-labeled liposomes have been used to image labeled stem cells with MRI.[46,61] Studies to date suggest that these MR-detectable probes are well tolerated by the stem cells and do not produce a decrease in their survival.[46,61] The principal limitation of cell labeling, however, is that no information regarding cell survival is obtained.[62] Magnetic resonance imaging reporter–based techniques are being developed to image cell survival in vivo but are still investigational in comparison with other reporter techniques.[62] In the immediate future, MRI of labeled stem cells will thus likely be used to guide their injection, track their movement over time, and assess local and global changes in myocardial function because of their presence.[62]

CONCLUSIONS AND FUTURE OUTLOOK

Molecular MRI has the potential to become an extremely important tool in the cardiovascular MRI armamentarium. Molecular MRI is already playing an important role in basic science investigation and the development of novel pharmaceuticals. In the near future, molecular MRI has the promise of making the early detection of clinical disease (eg, early atheroma and transplant rejection) possible and facilitating the use of personalized therapeutic regimens. Molecular MRI will provide complementary information to that provided by genomic and proteomic readouts but will allow the local extent and impact of a biological process to be determined without the confounding influence of factors elsewhere in the body. The translation of targeted molecular imaging agents into clinical use will be cautious and thorough, but several molecular MRI agents have already been used safely in humans.

Nuclear imaging of targeted ligands allows low doses of the ligand to be used, a distinct advantage in clinical translation. However, the attributes of MRI make it uniquely suited to the imaging of the cardiovascular system, and the integration of molecular MRI with anatomical and physiological MR data sets is thus highly compelling. The integration of molecular MRI

of the myocardium with spectroscopy, cine, delayed enhancement, and perfusion and strain imaging, for instance, constitutes a uniquely broad and powerful diagnostic arsenal.

Several molecular MRI imaging agents have already been successfully used in humans. The MNP ferumoxides (Feridex; Advanced Magnetics) has been clinically approved for liver imaging since 1993. The long-circulating MNP Combidex (Advanced Magnetics) has been used in humans to image lymph node metastases (phase 3 trials completed)[21] and is likely to gain full clinical approval in the near future. Combidex has also been used, although to a lesser extent, to image macrophage content in carotid atherosclerosis in humans.[51,52] A novel intravascular gadolinium chelate with high affinity for albumin is currently approved for clinical use in Europe.[63] In addition, a gadolinium chelate labeled with a fibrin-detecting peptide was recently used to detect thrombus, including intracardiac thrombus, in several clinical patients at 3 T.[55] Composite MRI of the atria, ventricles, aorta, and carotids could be achieved with this agent to detect the source of thrombus in these patients.[55] The initial experience with this fibrin-detecting probe in humans clearly demonstrates the feasibility and use of molecular MRI in the clinical setting.

Although molecular MRI will likely have the sensitivity to image many important processes, dual-modality strategies, such as MR-PET and MR-fluorescence,[27,64] will also be actively pursued. Combination MR-PET scanners are now being produced for human imaging and will allow MR and PET imaging to be performed simultaneously, rather than sequentially as done with PET–computed tomography. Advances in imaging hardware will be accompanied by advances in imaging agent design and the synthesis of agents with relaxivities significantly higher than present constructs. Molecular MRI is thus well poised to make an impact in all aspects of clinical care ranging from early screening to personalized therapy in advanced and established disease.

Acknowledgements

The author has been funded in part by National Institutes of Health Grants K08HL079984 and U01HL080731.

References

1. Sosnovik DE, Nahrendorf M, Weissleder R. Molecular magnetic resonance imaging in cardiovascular medicine. Circulation 2007;115:2076–2086. [PubMed: 17438163]
2. Jaffer FA, Libby P, Weissleder R. Molecular and cellular imaging of atherosclerosis: emerging applications. J Am Coll Cardiol 2006;47:1328–1338. [PubMed: 16580517]
3. Wu JC, Bengel FM, Gambhir SS. Cardiovascular molecular imaging. Radiology 2007;244:337–355. [PubMed: 17592037]
4. Weissleder R, Ntziachristos V. Shedding light onto live molecular targets. Nat Med 2003;9:123–128. [PubMed: 12514725]
5. Botnar RM, Perez AS, Witte S, et al. In vivo molecular imaging of acute and subacute thrombosis using a fibrin-binding magnetic resonance imaging contrast agent. Circulation 2004;109:2023–2029. [PubMed: 15066940]
6. Caravan P, Das B, Dumas S, et al. Collagen-targeted MRI contrast agent for molecular imaging of fibrosis. Angew Chem Int Ed Engl 2007;46:8171–8173. [PubMed: 17893943]
7. Frias JC, Williams KJ, Fisher EA, et al. Recombinant HDL-like nanoparticles: a specific contrast agent for MRI of atherosclerotic plaques. J Am Chem Soc 2004;126:16316–16317. [PubMed: 15600321]
8. Winter PM, Neubauer AM, Caruthers SD, et al. Endothelial alpha(v)beta3 integrin-targeted fumagillin nanoparticles inhibit angiogenesis in atherosclerosis. Arterioscler Thromb Vasc Biol 2006;26:2103–2109. [PubMed: 16825592]
9. Frias JC, Ma Y, Williams KJ, et al. Properties of a versatile nanoparticle platform contrast agent to image and characterize atherosclerotic plaques by magnetic resonance imaging. Nano Lett 2006;6:2220–2224. [PubMed: 17034087]

10. Amirbekian V, Lipinski MJ, Briley-Saebo KC, et al. Detecting and assessing macrophages in vivo to evaluate atherosclerosis noninvasively using molecular MRI. Proc Natl Acad Sci U S A 2007;104:961–966. [PubMed: 17215360]
11. Shen T, Weissleder R, Papisov M, et al. Monocrystalline iron oxide nanocompounds (MION): physicochemical properties. Magn Reson Med 1993;29:599–604. [PubMed: 8505895]
12. Wunderbaldinger P, Josephson L, Weissleder R. Crosslinked iron oxides (CLIO): a new platform for the development of targeted MR contrast agents. Acad Radiol 2002;9(suppl 2):S304–S306. [PubMed: 12188255]
13. Morawski AM, Winter PM, Crowder KC, et al. Targeted nanoparticles for quantitative imaging of sparse molecular epitopes with MRI. Magn Reson Med 2004;51:480–486. [PubMed: 15004788]
14. Sosnovik DE, Schellenberger EA, Nahrendorf M, et al. Magnetic resonance imaging of cardiomyocyte apoptosis with a novel magneto-optical nanoparticle. Magn Reson Med 2005;54:718–724. [PubMed: 16086367]
15. Nahrendorf M, Jaffer FA, Kelly KA, et al. Noninvasive vascular cell adhesion molecule–1 imaging identifies inflammatory activation of cells in atherosclerosis. Circulation 2006;114:1504–1511. [PubMed: 17000904]
16. Sosnovik DE, Dai G, Nahrendorf M, et al. Cardiac MRI in mice at 9.4 Tesla with a transmit-receive surface coil and a cardiac-tailored intensity-correction algorithm. J Magn Reson Imaging 2007;26:279–287. [PubMed: 17654729]
17. Li W, Salanitri J, Tutton S, et al. Lower extremity deep venous thrombosis: evaluation with ferumoxytol-enhanced MR imaging and dual-contrast mechanism—preliminary experience. Radiology 2007;242:873–881. [PubMed: 17325072]
18. Heyn C, Bowen CV, Rutt BK, et al. Detection threshold of single SPIO-labeled cells with FIESTA. Magn Reson Med 2005;53:312–320. [PubMed: 15678551]
19. Farrar CT, Dai G, Novikov M, et al. Impact of field strength and iron oxide nanoparticle concentration on the linearity and diagnostic accuracy of off-resonance imaging. NMR Biomed. 2007epub
20. Stuber M, Gilson WD, Schar M, et al. Positive contrast visualization of iron oxide-labeled stem cells using inversion-recovery with ON-resonant water suppression (IRON). Magn Reson Med 2007;58:1072–1077. [PubMed: 17969120]
21. Harisinghani MG, Barentsz J, Hahn PF, et al. Noninvasive detection of clinically occult lymph-node metastases in prostate cancer. N Engl J Med 2003;348:2491–2499. [PubMed: 12815134]
22. Moffat BA, Reddy GR, McConville P, et al. A novel polyacrylamide magnetic nanoparticle contrast agent for molecular imaging using MRI. Mol Imaging 2003;2:324–332. [PubMed: 14717331]
23. Weissleder R, Stark DD, Engelstad BL, et al. Superparamagnetic iron oxide: pharmacokinetics and toxicity. AJR Am J Roentgenol 1989;152:167–173. [PubMed: 2783272]
24. Wunderbaldinger P, Josephson L, Weissleder R. Tat peptide directs enhanced clearance and hepatic permeability of magnetic nanoparticles. Bioconjug Chem 2002;13:264–268. [PubMed: 11906263]
25. Jaffer FA, Nahrendorf M, Sosnovik D, et al. Cellular imaging of inflammation in atherosclerosis using magnetofluorescent nanomaterials. Mol Imaging 2006;5:85–92. [PubMed: 16954022]
26. Sosnovik DE, Nahrendorf M, Deliolanis N, et al. Fluorescence tomography and magnetic resonance imaging of myocardial macrophage 67 infiltration in infarcted myocardium in vivo. Circulation 2007;115:1384–1391. [PubMed: 17339546]
27. Kircher MF, Mahmood U, King RS, et al. A multimodal nanoparticle for preoperative magnetic resonance imaging and intraoperative optical brain tumor delineation. Cancer Res 2003;63:8122–8125. [PubMed: 14678964]
28. Schellenberger EA, Sosnovik D, Weissleder R, et al. Magneto/optical annexin V, a multimodal protein. Bioconjug Chem 2004;15:1062–1067. [PubMed: 15366960]
29. Winter PM, Morawski AM, Caruthers SD, et al. Molecular imaging of angiogenesis in early-stage atherosclerosis with alpha(v)beta3-integrin–targeted nanoparticles. Circulation 2003;108:2270–2274. [PubMed: 14557370]
30. Montet X, Montet-Abou K, Reynolds F, et al. Nanoparticle imaging of integrins on tumor cells. Neoplasia 2006;8:214–222. [PubMed: 16611415]

31. van Tilborg GA, Mulder WJ, Chin PT, et al. Annexin A5–conjugated quantum dots with a paramagnetic lipidic coating for the multimodal detection of apoptotic cells. Bioconjug Chem 2006;17:865–868. [PubMed: 16848390]
32. Kelly KA, Nahrendorf M, Yu AM, et al. In vivo phage display selection yields atherosclerotic plaque targeted peptides for imaging. Mol Imaging Biol 2006;8:201–207. [PubMed: 16791746]
33. Weissleder R, Kelly K, Sun EY, et al. Cell-specific targeting of nanoparticles by multivalent attachment of small molecules. Nat Biotechnol 2005;23:1418–1423. [PubMed: 16244656]
34. Sun EY, Josephson L, Kelly KA, et al. Development of nanoparticle libraries for biosensing. Bioconjug Chem 2006;17:109–113. [PubMed: 16417258]
35. Sirol M, Itskovich VV, Mani V, et al. Lipid-rich atherosclerotic plaques detected by gadofluorine-enhanced in vivo magnetic resonance imaging. Circulation 2004;109:2890–2896. [PubMed: 15184290]
36. Meding J, Urich M, Licha K, et al. Magnetic resonance imaging of atherosclerosis by targeting extracellular matrix deposition with gadofluorine M. Contrast Media Mol Imaging 2007;2:120–129. [PubMed: 17557276]
37. Hogemann-Savellano D, Bos E, Blondet C, et al. The transferrin receptor: a potential molecular imaging marker for human cancer. Neoplasia 2003;5:495–506. [PubMed: 14965443]
38. Taktak S, Sosnovik D, Cima MJ, et al. Multiparameter magnetic relaxation switch assays. Anal Chem 2007;79:8863–8869. [PubMed: 17983206]
39. Perez JM, Josephson L, O'Loughlin T, et al. Magnetic relaxation switches capable of sensing molecular interactions. Nat Biotechnol 2002;20:816–820. [PubMed: 12134166]
40. Heyn C, Ronald JA, Ramadan SS, et al. In vivo MRI of cancer cell fate at the single-cell level in a mouse model of breast cancer metastasis to the brain. Magn Reson Med 2006;56:1001–1010. [PubMed: 17029229]
41. Cunningham CH, Arai T, Yang PC, et al. Positive contrast magnetic resonance imaging of cells labeled with magnetic nanoparticles. Magn Reson Med 2005;53:999–1005. [PubMed: 15844142]
42. Mani V, Briley-Saebo KC, Itskovich VV, et al. Gradient echo acquisition for superparamagnetic particles with positive contrast (GRASP): sequence characterization in membrane and glass superparamagnetic iron oxide phantoms at 1.5T and 3T. Magn Reson Med 2006;55:126–135. [PubMed: 16342148]
43. Stuber M, Gilson W, Schaer M, et al. Shedding light on the dark spot with IRON—a method that generates positive contrast in the presence of superparamagnetic nanoparticles. Proc Intl Soc Magn Reson Med 2005;13:2608.
44. Vaughan T, DelaBarre L, Snyder C, et al. 9.4T human MRI: preliminary results. Magn Reson Med 2006;56:1274–1282. [PubMed: 17075852]
45. Caruthers SD, Neubauer AM, Hockett FD, et al. In vitro demonstration using 19F magnetic resonance to augment molecular imaging with paramagnetic perfluorocarbon nanoparticles at 1.5 Tesla. Invest Radiol 2006;41:305–312. [PubMed: 16481914]
46. Partlow KC, Chen J, Brant JA, et al. 19F magnetic resonance imaging for stem/progenitor cell tracking with multiple unique perfluorocarbon nanobeacons. FASEB J 2007;21:1647–1654. [PubMed: 17284484]
47. Aime S, Carrera C, Delli Castelli D, et al. Tunable imaging of cells labeled with MRI-PARACEST agents. Angew Chem Int Ed Engl 2005;44:1813–1815. [PubMed: 15723362]
48. Woods M, Woessner DE, Sherry AD. Paramagnetic lanthanide complexes as PARACEST agents for medical imaging. Chem Soc Rev 2006;35:500–511. [PubMed: 16729144]
49. Barkhausen J, Ebert W, Heyer C, et al. Detection of atherosclerotic plaque with gadofluorine-enhanced magnetic resonance imaging. Circulation 2003;108:605–609. [PubMed: 12835227]
50. Schmitz SA, Taupitz M, Wagner S, et al. Iron-oxide–enhanced magnetic resonance imaging of atherosclerotic plaques: postmortem analysis of accuracy, inter-observer agreement, and pitfalls. Invest Radiol 2002;37:405–411. [PubMed: 12068163]
51. Kooi ME, Cappendijk VC, Cleutjens KB, et al. Accumulation of ultrasmall superparamagnetic particles of iron oxide in human atherosclerotic plaques can be detected by in vivo magnetic resonance imaging. Circulation 2003;107:2453–2458. [PubMed: 12719280]

52. Trivedi RAJMUK-I, Graves MJ, et al. In vivo detection of macrophages in human carotid atheroma: temporal dependence of ultrasmall superparamagnetic particles of iron oxide-enhanced MRI. Stroke 2004;35:1631–1635. [PubMed: 15166394]

53. Mani V, Briley-Saebo KC, Hyafil F, et al. Feasibility of in vivo identification of endogenous ferritin with positive contrast MRI in rabbit carotid crush injury using GRASP. Magn Reson Med 2006;56:1096–1106. [PubMed: 17036302]

54. Winter PM, Caruthers SD, Yu X, et al. Improved molecular imaging contrast agent for detection of human thrombus. Magn Reson Med 2003;50:411–416. [PubMed: 12876719]

55. Katoh M, Wiethoff A, Sparing R, et al. Molecular MRI of thrombosis using novel fibrin-specific contrast agent: initial results in humans at 3.0 T. Proc Intl Soc Mag Reson 2007;9:100.

56. Hiller KH, Waller C, Nahrendorf M, et al. Assessment of cardiovascular apoptosis in the isolated rat heart by magnetic resonance molecular imaging. Mol Imaging 2006;5:115–121. [PubMed: 16954025]

57. Weissleder R, Lee AS, Khaw BA, et al. Antimyosin-labeled monocrystalline iron oxide allows detection of myocardial infarct: MR antibody imaging. Radiology 1992;182:381–385. [PubMed: 1732953]

58. Kanno S, Wu YJ, Lee PC, et al. Macrophage accumulation associated with rat cardiac allograft rejection detected by magnetic resonance imaging with ultrasmall superparamagnetic iron oxide particles. Circulation 2001;104:934–938. [PubMed: 11514382]

59. Nahrendorf M, Sosnovik DE, Waterman P, et al. Dual channel optical tomographic imaging of leukocyte recruitment and protease activity in the healing myocardial infarct. Circ Res 2007;100:1218–1225. [PubMed: 17379832]

60. Chen JW, Querol Sans M, Bogdanov A Jr, et al. Imaging of myeloperoxidase in mice by using novel amplifiable paramagnetic substrates. Radiology 2006;240:473–481. [PubMed: 16864673]

61. Kraitchman DL, Heldman AW, Atalar E, et al. In vivo magnetic resonance imaging of mesenchymal stem cells in myocardial infarction. Circulation 2003;107:2290–2293. [PubMed: 12732608]

62. Zhou R, Acton PD, Ferrari VA. Imaging stem cells implanted in infarcted myocardium. J Am Coll Cardiol 2006;48:2094–2106. [PubMed: 17112999]

63. Shamsi K, Yucel EK, Chamberlin P. A summary of safety of gadofosveset (MS-325) at 0.03 mmol/kg body weight dose: phase II and phase III clinical trials data. Invest Radiol 2006;41:822–830. [PubMed: 17035873]

64. Pichler BJ, Judenhofer MS, Catana C, et al. Performance test of an LSO-APD detector in a 7-T MRI scanner for simultaneous PET/MRI. J Nucl Med 2006;47:639–647. [PubMed: 16595498]

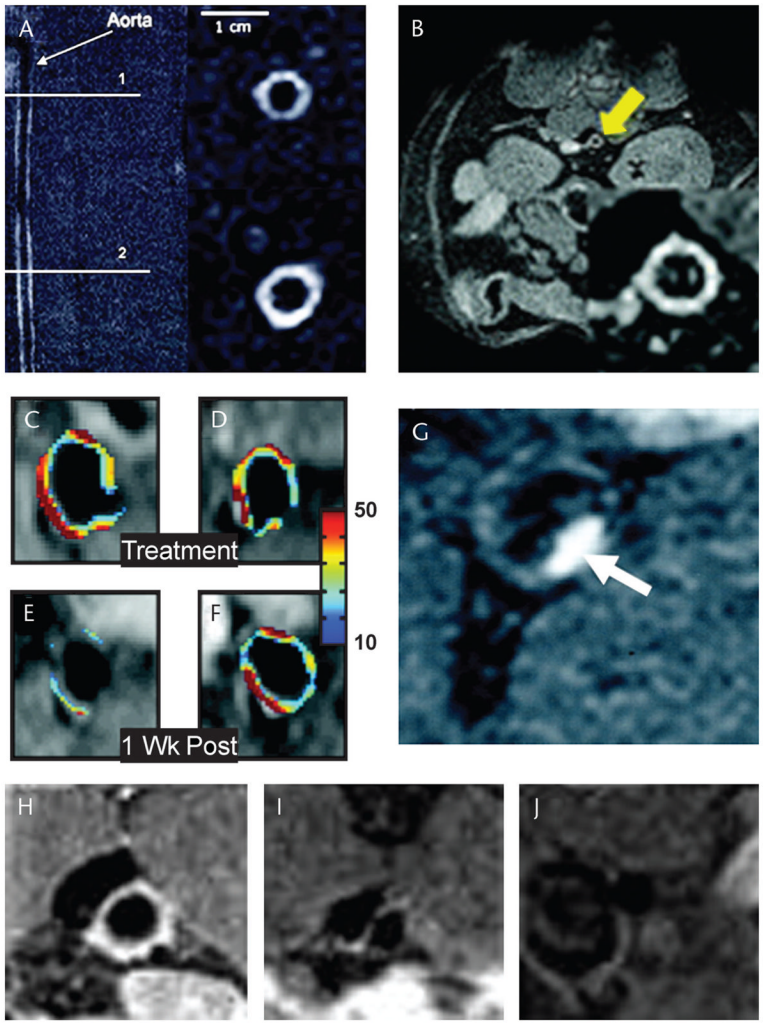

FIGURE 1.

Imaging of atherosclerosis with paramagnetic gadolinium-based imaging agents: gadofluorine accumulates in the matrix of atheromatous plaques but not in normal portions of the arterial wall (A).[35] Reproduced with permission from Sirol et al.[35] Gadolinium-containing HDL-like nanoparticles accumulate preferentially in lipid and macrophage rich atherosclerotic plaques (B).[7] Reproduced with permission from Frias et al.[7] Angiogenesis in atherosclerotic plaques can be imaged with a gadolinium-containing liposome targeted to the $\alpha_v\beta_3$ integrin (C, D).8 When the antiangiogenic agent fumagillin is incorporated into the liposome, it produces a significant subsequent reduction in plaque neovascularization (E), not seen in plaques targeted with control liposomes (F).[8] Reproduced with permission from Winter et al.[8] Plaque thrombosis can be imaged in vivo with a fibrin-targeted small gadolinium chelate (G).[5] Reproduced with permission from Botnar et al.[5] A gadolinium-containing immunomicelle targeted to the macrophage scavenger receptor (H–J).[10] Labeled immunomicelles (H) imaged 24 hours after injection produce significant enhancement of atherosclerotic plaques in the aorta of apoE$^{-/-}$ mice, whereas nonlabeled immunomicelles (I) and gadolinium–diethylenetriamine pentaacetic acid (J) do not. Reproduced with permission from Amirbekian et al.[10]

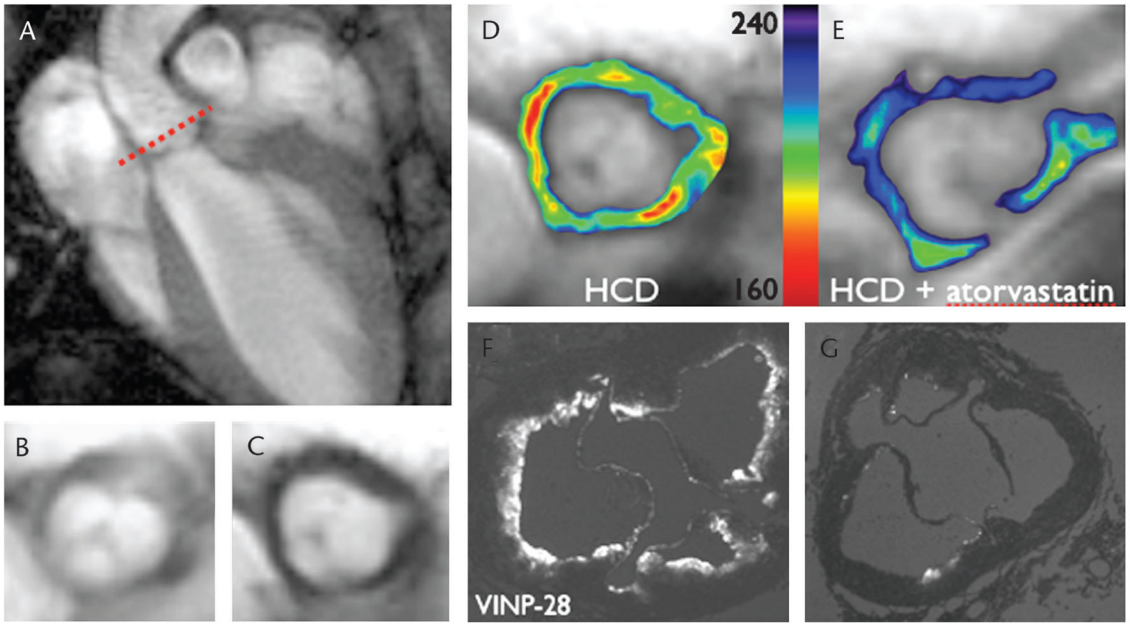

FIGURE 2.

Molecular MRI of VCAM-1 expression in apoE$^{-/-}$ mice.[15] The MNP CLIO-Cy5.5 has been labeled with a peptide with high affinity and specificity for VCAM-1. T2*-weighted gradient echo image in the long axis of the left ventricle and thoracic aorta (A). The short-axis plane through the aortic root, an area of high plaque burden, is shown by the dashed line. Short-axis images (B, C) of the aortic root before (B) and after (C) the injection of the probe are shown. Significant negative contrast, consistent with VCAM-1 expression and accumulation of the probe, is seen. Vascular cell adhesion molecule 1 expression (D, E) in the aortic root of a cholesterol-fed apoE$^{-/-}$ mouse (D) is shown by in vivo MRI to be significantly higher than that of an identical statin-treated apoE$^{-/-}$ mouse (E). Ex vivo fluorescence images of the aortic root confirm the in vivo MRI findings with significantly more probe accumulation seen in the untreated mouse (F) than in the statin-treated mouse (G).[15]

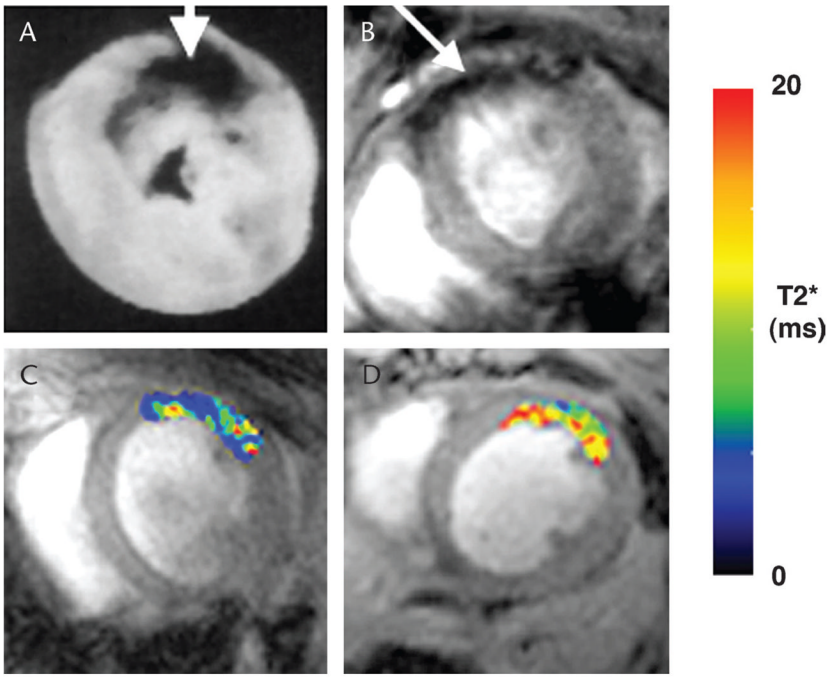

FIGURE 3.

Molecular MRI of cardiomyocyte apoptosis and necrosis. Ex vivo MRI of antimyosin-labeled MION in myocardial infarction in rats (A).[57] Accumulation of the probe produces negative contrast in the infarcted myocardium. Molecular MRI of cardiomyocyte apoptosis in mice with ischemia-reperfusion injury (B–D).[14] The mice were injected with the annexin-labeled MNP, AnxCLIO-Cy5.5, after transient ligation of the left coronary artery. Accumulation of the agent was seen in the hypokinetic anterior wall of all mice injected with AnxCLIO-Cy5.5 (B, arrow).[14] No significant accumulation of the unlabeled control probe, CLIO-Cy5.5, was seen in the myocardium in any of the mice. In vivo T2* maps created in regions of interest defined by the area of hypokinesis in the anterolateral wall of the myocardium after ischemia-reperfusion (C, D). Significantly greater probe accumulation (lower T2* values) was seen in mice injected with AnxCLIO-Cy5.5 (C) than in mice injected with the unlabeled control probe CLIO-Cy5.5 (D).[14]

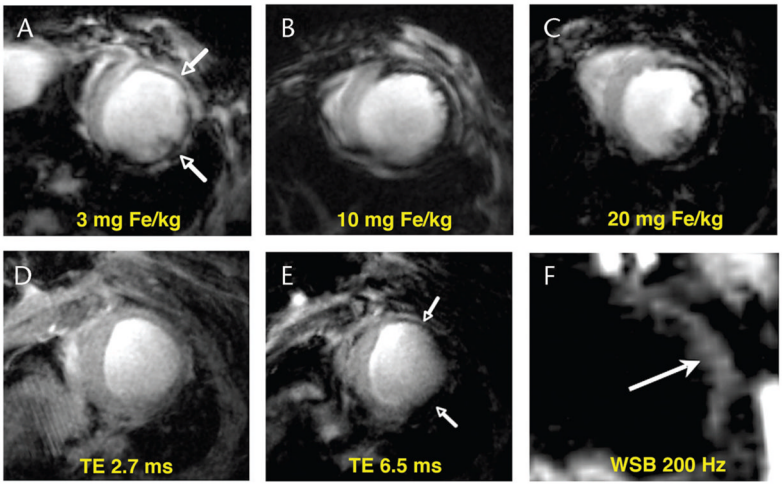

FIGURE 4.

Conventional T2* gradient echo and off-resonance imaging of postinfarction myocardial macrophage infiltration.[19,26] Mice injected with doses of CLIO-Cy5.5, ranging from 3 to 20 mg Fe/kg, 48 hours after infarction (A–C). Imaging was performed a further 48 hours later (96 hours after infarction). Accumulation of the agent in macrophages infiltrating the healing infarct produced marked signal hypointensity (negative contrast) in the injured anterolateral wall (arrows).[26] A clear and linear dose response between the degree of contrast in the myocardium and the dose of the agent injected was seen.[26] T2*-weighted gradient echo imaging (D, E) in a mouse injected with 20 mg Fe/kg of CLIO-Cy5.5 48 hours after infarction and imaged a further 48 hours later[26]; TE, 2.7 milliseconds (D), and TE, 6.5 milliseconds (E). The thinned infarcted anterolateral wall is clearly seen at the shortest TE and develops negative contrast, because of MNP accumulation, only once the TE is increased.[26] Off-resonance imaging of postinfarction macrophage infiltration with an on-resonance water suppression bandwidth of 200 Hz (F).[19] Iron oxide accumulation in the anterolateral wall shifts local spins off-resonance producing positive contrast.

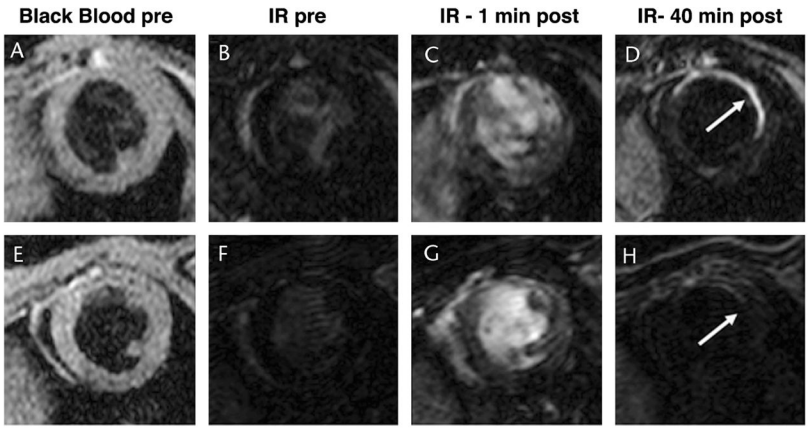

FIGURE 5.

Molecular MRI of myocardial fibrosis with a gadolinium chelate targeted to collagen type 1.[6] Chelate labeled with targeted peptide (A–D). Chelate labeled with isomer of targeted peptide (E–H). Images from a mouse injected with the active agent on day 40 after infarction (A–D) and with the control agent 2 days later (E–H) are shown. Sustained accumulation of the targeted chelate is seen in the infarcted anterolateral wall (D). Only minimal uptake of the control (isomer-labeled) probe is seen (H). Reproduced with permission from Caravan et al.[6] IR indicates T1-weighted inversion recovery sequence to null normal myocardium.

TABLE 1

Potential Artifacts With Iron Oxide Nanoparticles in Cardiovascular Molecular MRI

	Iron Oxide MNPs	
Artifact	**Potential Error**	**Solution**
Calcification	Low signal may mimic MNP uptake	MNPs produces bright signal with T1 and off-resonance techniques. Ultrashort echo or UTE techniques may also play a role
Air	Low signal may mimic MNP uptake	MNPs produces bright signal with T1 and off-resonance techniques. Ultrashort echo or UTE techniques may also play a role
Susceptibility Artifacts	Can produce either negative or positive contrast depending on whether on- or off-resonance techniques are used	Compare with conventional T1- and T2-weighted spin echo images
Hemorrhage	Endogenous iron products may mimic exogenous MNP accumulation.	Contrast consistent with presence of iron is present before the injection of the exogenous agent. Dual modality imaging (MRI-fluorescence or MR-PET) may be needed
Motion	Can produce spin dephasing and MR signal loss, particularly with the long TEs needed for T2* weighting	Reduce TE of T2*-weighted image, use gradient moment nulling, change to off-resonance technique where short TEs are integral and advantageous

UTE indicates ultrashort TE.

TABLE 2

Potential Artifacts With Gadolinium-Based Agents in Cardiovascular Molecular MRI

	Gadolinium Constructs	
Artifact	**Potential Error**	**Solution**
Incomplete fat suppression	Short T1 of fat may mimic probe uptake in the vessel wall or subepicardium.	Improve shim or use inversion recovery techniques for fat saturation
Incomplete suppression of signal from blood pool due to slow flow	Residual positive signal from blood pool may mimic probe uptake in atherosclerotic plaque and in the subendocardium.	Use of strong diffusion gradients, often with a stimulated echo sequence, to produce robust black blood effect even with slow flow.
B1 Inhomogeneity	Variable flip angle can produce inconsistent T1 contrast in image. Problem only in humans and larger animals at higher field strengths	Adiabatic excitation pulses or RF shimming with transmit arrays (multiple individual transmit coils and channels)
Poor breath-hold	Ghosting from chest wall fat can produce signal overlying the heart.	Parallel acquisition to reduce breath-hold duration and/or use of fat suppression

RF indicates radiofrequency.